Cell Metabolism
Article

Insulin Activates Erk1/2 Signaling in the Dorsal Vagal Complex to Inhibit Glucose Production

Beatrice M. Filippi,[1,2] Clair S. Yang,[1,3] Christine Tang,[1] and Tony K.T. Lam[1,2,3,4,*]
[1]Toronto General Research Institute, University Health Network, Toronto, M5G 1L7, Canada
[2]Department of Medicine
[3]Department of Physiology
University of Toronto, Toronto, M5S 1A8, Canada
[4]Banting and Best Diabetes Centre, University of Toronto, Toronto, M5G 2C4, Canada
*Correspondence: tony.lam@uhnres.utoronto.ca
http://dx.doi.org/10.1016/j.cmet.2012.09.005

SUMMARY

Insulin activates PI3-kinase (PI3K)/AKT to regulate glucose homeostasis in the peripheral tissues and the mediobasal hypothalamus (MBH) of rodents. We report that insulin infusion into the MBH or dorsal vagal complex (DVC) activated insulin receptors. The same dose of insulin that activated MBH PI3K/AKT did not in the DVC. DVC insulin instead activated Erk1/2 and lowered glucose production in rats and mice. Molecular and chemical inhibition of DVC Erk1/2 negated, while activation of DVC Erk1/2 recapitulated, the effects of DVC insulin. Circulating insulin failed to inhibit glucose production when DVC Erk1/2 was inhibited in normal rodents, while DVC insulin action was disrupted in high-fat-fed rodents. Activation of DVC ATP-sensitive potassium channels was necessary for insulin-Erk1/2 and sufficient to inhibit glucose production in normal and high-fat-fed rodents. DVC is a site of insulin action where insulin triggers Erk1/2 signaling to inhibit glucose production and of insulin resistance in high-fat feeding.

INTRODUCTION

Hepatic insulin resistance is a hallmark feature of diabetes and obesity (Defronzo, 2009) and is defined as the inability of insulin to inhibit hepatic glucose production, leading to a dysregulation of glucose homeostasis. The inability of circulating hyperinsulinemia to inhibit glucose production in obesity and diabetes is due in part to a direct disruption of insulin signaling cascades in the liver (Saltiel and Kahn, 2001). Recent studies, however, implicate that insulin resistance in the MBH leads to a dysregulation of glucose production and homeostasis in diabetes and obesity as well (Gelling et al., 2006; Ono et al., 2008).

In this regard, central administration of insulin is first documented to lower plasma glucose levels in normal dogs (Agarwala et al., 1977; Chowers et al., 1966), and this glucose-lowering effect is abolished only when the liver is removed (Agarwala et al., 1977). In parallel, direct infusion of insulin into the hypothalamus of normal rats lowers plasma glucose levels through an inhibition of hepatic glucose production (Obici et al., 2002; Pocai et al., 2005). Although the insulin signaling cascades in the hypothalamus remain elusive, studies in rodents report that the activation of the hypothalamic insulin receptor → PI3-kinase (PI3K) → ATP-sensitive potassium (K_{ATP}) channels signaling is necessary for insulin to inhibit glucose production (Könner et al., 2007a; Obici et al., 2002; Pocai et al., 2005). Importantly, central delivery of insulin (Hallschmid et al., 2012; Filippi et al., 2012) as well as activation of K_{ATP} channels in the brain (Kishore et al., 2011) are implicated to lower plasma glucose levels and glucose production in humans as well, although central insulin regulates net hepatic glucose uptake rather than glucose production in dogs (Ramnanan et al., 2011). Nonetheless, the significance of these findings as a whole is anchored when high-fat feeding disrupts hypothalamic insulin signaling through the activation of S6 kinase to inhibit glucose production (Ono et al., 2008), while insulin injection triggers PI3K-AKT signaling in the hypothalamus to lower glucose concentrations in uncontrolled diabetic rats (Gelling et al., 2006).

It is crucial to continue dissecting the hypothalamic insulin signaling cascades that regulate peripheral metabolism. However, studies aiming to assess whether extra-hypothalamic regions are sensitive to insulin to regulate glucose homeostasis are equally important to potentially reveal signaling mechanisms in the brain that mediate insulin action/resistance. DVC is an extra-hypothalamic region that integrates nutritional and hormonal signals to regulate peripheral metabolism (Coll et al., 2007; Cummings and Overduin, 2007; Grill, 2006; Morton et al., 2005). In particular, a study reports that insulin injection into the brainstem may inhibit food intake by decreasing the expression of the Hap1-Ahi1 complex in mice (Niu et al., 2011), but the potential impact of insulin on glucose regulation remains unknown. In parallel, activation of *N*-Methyl-d-aspartate (NMDA) receptor in the DVC is sufficient (Lam et al., 2010a) and necessary for nutrient sensing mechanisms in the gut (Breen et al., 2012; Cheung et al., 2009; Wang et al., 2008) and the hypothalamus (Lam et al., 2011) to inhibit glucose production and regulate glucose homeostasis. These studies collectively

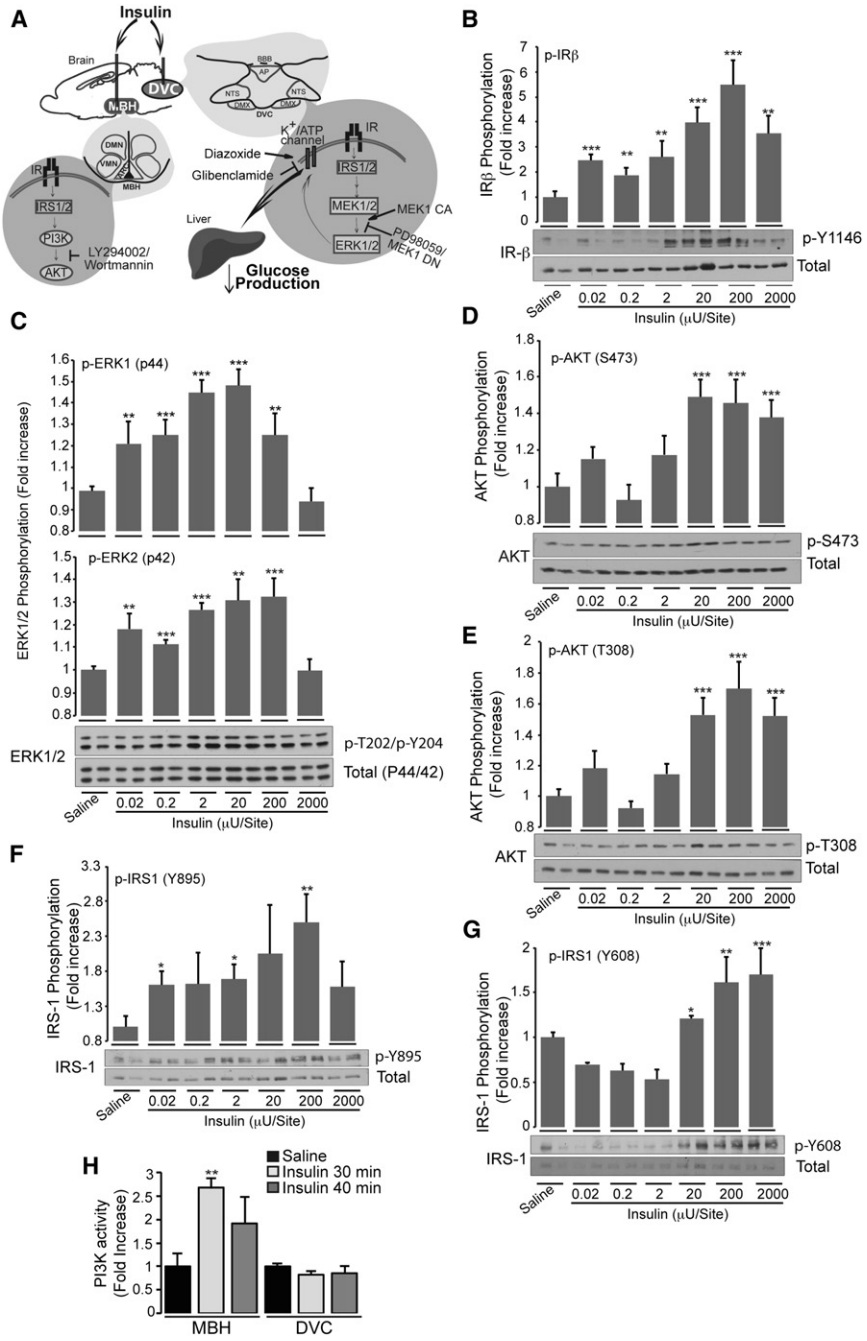

Figure 1. Insulin Signaling in the DVC

(A) Schematic representation of the working hypothesis: Insulin action in the DVC and MBH activates diverging signaling pathways that lead to the activation of the K_{ATP} channels to inhibit glucose production. The signaling cascade involves MEK1/2/ERK1/2 in the DVC and PI3K in the MBH.

(B–G) The indicated amounts of insulin were infused for 5 min (0.2 μl/min) bilaterally into the DVC of rats that were sacrificed after 30 min. The level of phosphorylation of the IRβ (B), Erk1/2 (C), AKT (D, E), and IRS-1 (F, G) were analyzed by western blot. The phosphorylation level was quantified by densitometry and normalized for the total protein. For each condition n = 4 samples were analyzed. Data are presented as fold increase over the saline-treated samples. A representative blot for each protein is shown.

(H) The PI3K activity in both MBH and DVC tissues upon insulin (0.2 μl/min for 5 min, 2 μU/site) stimulation is shown. The PI3K (p85 subunit) was immunoprecipitated from 500 μg of tissue and its activity analyzed with the PI3K activity ELISA kit. For each condition, n = 5 (DVC) or n = 6 (MBH) rats were analyzed. Data are presented as fold increase over the saline-treated samples. **p < 0.01, *p < 0.05 versus corresponding control.

underscore the possibility that insulin triggers signaling pathways in the DVC to regulate glucose production and glucose homeostasis.

Here, we assessed whether insulin infusion in the DVC activates the canonical PI3K-AKT signaling pathway or the alternative dual specificity kinase MAPK kinase (MEK1/2) pathway that phosphorylates direct effectors Erk1 and Erk2. Using both molecular and chemical gain- and loss-of-function approaches, we then evaluated the glucoregulatory impact of the signaling pathways activated by insulin in the DVC. Our findings unexpectedly illustrate that insulin triggers a PI3K-independent but MAP-dependent pathway in the DVC to inhibit glucose production (Figure 1A).

RESULTS

Insulin Signaling in the DVC

To first characterize the signaling pathways that are activated by insulin in the DVC, insulin (2 μU/site; 0.2 μl/min for 5 min; analogous to MBH studies [Ono et al., 2008]) was infused bilaterally into the DVC, targeting the nucleus of the solitary tract of conscious, unrestrained rats. DVC wedges were than collected after 5, 15, 30, 40, and 50 min. DVC insulin activated insulin receptor (assessed by phosphorylation of residue Y1146 in the β subunit, Figures S1A and S1B) but not AKT (assessed by phosphorylation of residue S473, Figure S1C) within 30–40 min of infusion. DVC insulin instead activated Erk1/2 (assessed by phosphorylation of residue T202 and residue Y204, Figure S1D) in the same time frame. In contrast to the DVC, MBH insulin (2 μU/site) activated insulin receptor (Figure S2A) and AKT (Figure S2B) but not Erk2 (Figure S2C). Erk1 phosphorylation was elevated by 40 min (but not 30 min) of MBH insulin infusion. These data indicate that insulin activates its receptor in both MBH and DVC. However, the same dose of insulin that activated downstream PI3K and AKT signaling in the MBH did not activate PI3K/AKT in the DVC. DVC insulin instead activated Erk1/2 signaling.

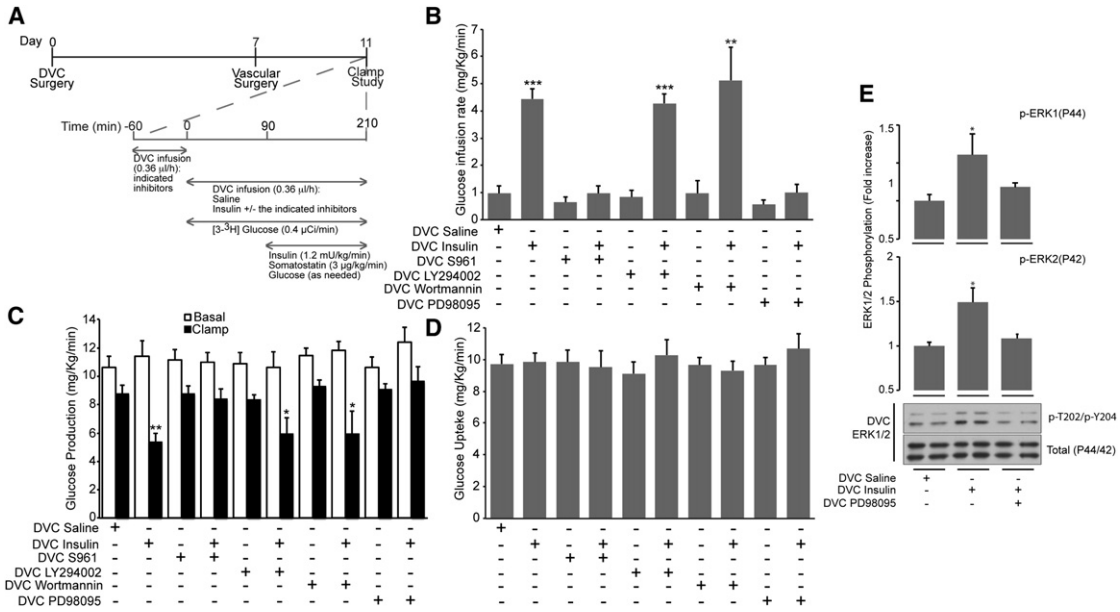

Figure 2. DVC Insulin Activates an Insulin Receptor-Erk1/2-Dependent but PI3K-Independent Pathway to Inhibit Glucose Production

(A) Experimental procedure and clamp protocol. Saline or insulin (a total of 2.52 μU, 1.26 μU per site) was infused at 0.006 μl/min during the clamp through the DVC catheter. The insulin receptor antagonist (S961, 1.3 μg/μl), PI3K inhibitors (LY294002, 10 μM and wortmannin, 2 μM), and the MEK1/2 inhibitor (PD98059, 100 μM) were preinfused at 0.006 μl/min for 1 hr before the clamp and then infused or coinfused with insulin during the clamp.

(B) Glucose infusion rate (mg/Kg/min) during the final 30 min of the clamp for the indicated treatment.

(C) Glucose production (mg/Kg/min) in basal (with square) and clamp (black square) conditions.

(D) Glucose uptake was comparable in all groups. Values are shown as mean + SEM; n = 6 for saline, insulin, and PD98059 + insulin treatments; n = 9 for S961 + insulin; and n = 4 for LY294002 + insulin, wortmannin + insulin, and S961, PD98059, LY294002, and wortmannin alone treatments.

(E) A total of 4 μU (2 per site) of insulin were infused bilaterally into the DVC for 5 min (0.4 μU/min). The MEK1/2 inhibitor (PD98059, 200 μM) was preinfused at 0.2 μl/min for 5 min and 1 hr before the insulin treatment, and then coinfused with insulin. The rats were then sacrificed after 30 min. The level of phosphorylation of the Erk1/2 was analyzed by western blot. The phosphorylation level was quantified by densitometry and normalized for the total protein. For each condition n = 5 samples were analyzed. Data are presented as fold increase over the saline-treated samples. A representative blot for each protein is shown. Values are shown as mean + SEM. ***p < 0.001, **p < 0.01, *p < 0.05 versus corresponding control.

We next performed an insulin dose-response study whereby insulin was infused into the DVC from 0.02 μU/site to 2 mU/site (Figures 1B–1G). DVC wedges were obtained 30 min after infusion. DVC insulin receptor was activated at 0.02, 0.2, and 2 μU/site and reached a peak at 20–200 μU/site (Figure 1B). We then discovered DVC Erk1/2 activation followed a trend similar to insulin receptor activation (Figure 1C). On the other hand, DVC insulin did not significantly activate AKT (assessed by the activatory phosphosite, S473, and T308) until reaching 20 μU/site (Figures 1D and 1E). In addition, we examined the IRS-1 phosphorylation level, in particular focusing on two phosphosites that lead specifically to the activation of Erk1/2 (Y895) and PI3K (Y608) (Figure 1G) (Sun and Liu, 2009). The pattern of the phosphorylation of the Y895 on IRS-1 (Figure 1F) directly reflected the response of Erk1/2 (Figure 1C), while the phosphorylation of the Y608 similarly followed the pattern of AKT activation (Figures 1D and 1E). Lastly, we measured PI3K activity where we immunoprecipitated the PI3K from both MBH and DVC wedges and measured the PIP3 production. Consistent with the effect on AKT (Figures S1 and S2), MBH but not DVC insulin infusion (2 μU/site) activated PI3K activity (Figure 1H). These findings collectively indicate that DVC insulin infused at 2 μU/site activated Erk1/2 but not PI3K-AKT signaling.

Insulin Action in the DVC Lowers Glucose Production in Rats and Mice

To address for a potential functional relevance of DVC insulin signaling on glucose regulation independent of changes in body weight (Table S1), insulin was first administered continuously into the DVC (0.006 μU/min, a total of 1.26 μU/site; analogous to MBH studies [Pocai et al., 2005]), targeting the nucleus of the solitary tract, while changes in steady-state glucose kinetics were assessed with the tracer-dilution methodology (Figure 2A). To ensure that any changes in glucose kinetics were not due to changes in circulating glucoregulatory hormones such as insulin and glucagon, the rats underwent the pancreatic-euglycemic clamps where plasma glucose and insulin levels were experimentally maintained at basal level (Tables S2 and S3). During the clamps, DVC insulin significantly increased the glucose infusion rate required to prevent hypoglycemia (Figure 2B). The drop in plasma glucose was due to an inhibition of glucose production (Figure 2C and Figure S3), rather than changes in glucose uptake (Figure 2D).

To evaluate whether DVC insulin also regulates glucose production in mice, we repeated the infusion clamp experiments in normal C57/B6 mice (Figure 3A). Mice underwent stereotactic surgery for a single catheter implantation that targeted the fourth ventricle as well as vascularization for infusion. Direct infusion of

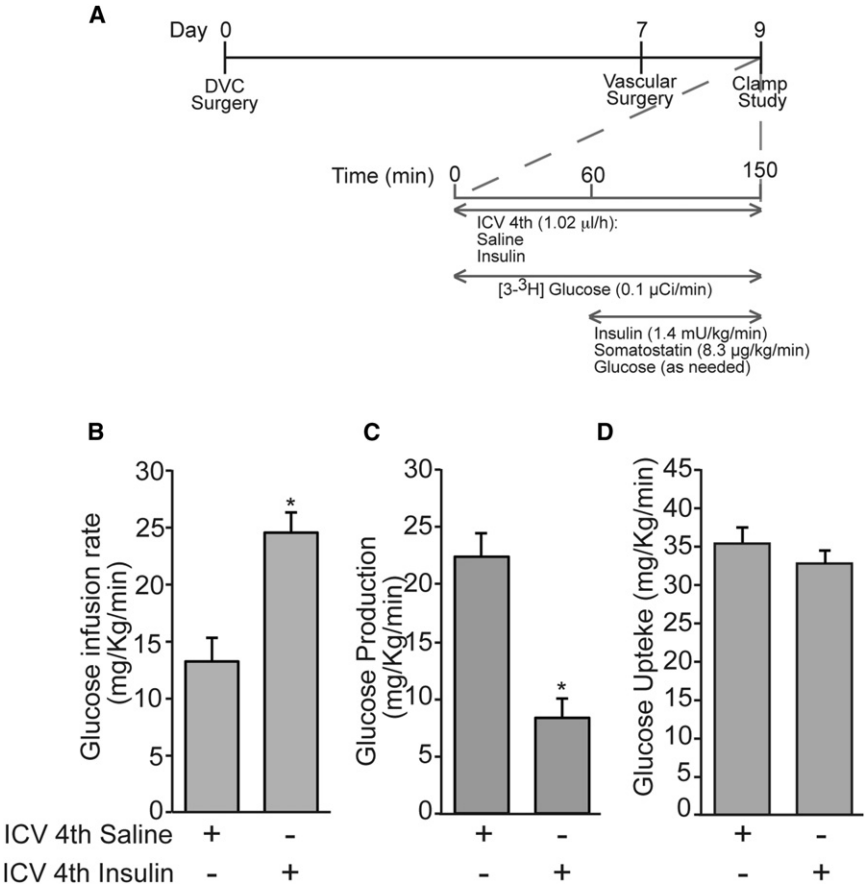

Figure 3. Intracerebroventricular (Fourth) Infusion of Insulin Lowers Glucose Production in Mice

(A) Experimental procedure and clamp protocol. Saline or insulin (a total of 4 μU) was infused at 0.017 μl/min during the clamp through the ICV (fourth) catheter.

(B) Glucose infusion rate (mg/Kg/min) measured during the final 20 min of the clamp.

(C) Glucose production (mg/Kg/min) during the clamp.

(D) Glucose uptake was comparable in all groups. Values are shown as mean + SEM n = 8 mice per group. *p < 0.05 versus corresponding control.

insulin versus saline into the fourth ventricle significantly increased the glucose infusion rate required to maintain euglycemia (Figure 3B). Consistent with data obtained in rats, insulin fourth ventricle inhibited glucose production (Figure 3C) but did not affect glucose uptake (Figure 3D) in mice. Together, these findings suggest that insulin action in the DVC inhibits glucose production in rats and mice in vivo.

To evaluate whether insulin receptor activation in the DVC is necessary for insulin action, an insulin receptor antagonist, S961 (Schäffer et al., 2008), was infused into the DVC in the presence or absence of insulin. Of note, a previous study documented the effectiveness of using S961 in negating insulin action in the ventromedial hypothalamus (Paranjape et al., 2010). Coinfusion of S961 with insulin in the DVC negated the ability of DVC insulin to increase glucose infusion rate (Figure 2B) and lower glucose production (Figure 2C and Figure S3). Glucose uptake was not affected (Figure 2D), and DVC S961 alone did not affect glucose metabolism (Figures 2B–2D and Figure S3). Thus, insulin activates insulin receptor in the DVC to lower glucose production.

Insulin Activates a DVC PI3K-Independent but Erk1/2-Dependent Pathway to Inhibit Glucose Production

To evaluate whether PI3K signaling is necessary for DVC insulin to inhibit glucose production, we coinfused DVC insulin with either PI3K inhibitor LY 294002 or wortmannin (Figure 2A). Neither of the PI3K inhibitors abolished the glucoregulatory effect of DVC insulin (Figures 2B and 2C), consistent with the fact that DVC insulin failed to activate PI3K-AKT signaling when administered at a dose (2 μU/site) similar to the clamp studies (Figures 1D, 1E, 1G, and 1H). DVC PI3K inhibitors alone did not affect glucose metabolism (Figures 2B–2D).

The activation of the insulin receptor by insulin also leads to the activation of a MAPK-dependent signaling pathway (Saltiel and Kahn, 2001), and DVC insulin activated Erk1/2 signaling (Figure 1C and Figure S1D). We next explored whether DVC insulin triggers MAPK signaling events to inhibit glucose production. When we coinfused the MEK1/2 inhibitor PD98059 with insulin in the DVC, the ability of DVC insulin to activate Erk1/2 (Figure 2E), increase glucose infusion rate (Figure 2B), and inhibit glucose production (Figure 2C) was negated. Glucose uptake was unaltered (Figure 2D), and DVC PD98059 alone did not affect glucose metabolism (Figures 2B–2D).

To alternatively evaluate for the role of DVC Erk1/2 signaling, an adenovirus expressing the dominant-negative form of MEK1 (MEK1-DN) was generated (Figure 4A). MEK1-DN negated insulin-induced Erk1/2 activation in HEK293 cell line, while insulin receptor and AKT activation were intact (Figure 4B). Direct injection of MEK1-DN into the DVC also negated insulin-induced Erk1/2 activation (Figure 4C). During the clamps, DVC MEK1-DN reversed the ability of DVC insulin infusion to increase glucose infusion rate (Figure 4D) and lower glucose production (Figure 4E and Figure S4A) as compared to DVC GFP-injected control rats. DVC MEK1-DN alone did not affect glucose regulation (Figures 4D and 4E and Figure S4A), and glucose uptake remained comparable among groups (Figure S4B).

We next activated DVC Erk1/2 signaling per se and evaluated whether the metabolic effect of insulin is recapitulated. An adenovirus expressing the constitutively active form of MEK1 (MEK1-CA) was constructed (Figure 4A) and was found to activate Erk1/2 signaling in vitro (Figure 4B). Direct injection of MEK1-CA into the DVC activated Erk1/2 signaling (Figure 4C) and was sufficient to increase glucose infusion rate (Figure 4D) and lower glucose production (Figure 4E and Figure S4A) during the clamps compared to DVC GFP-injected control rats.

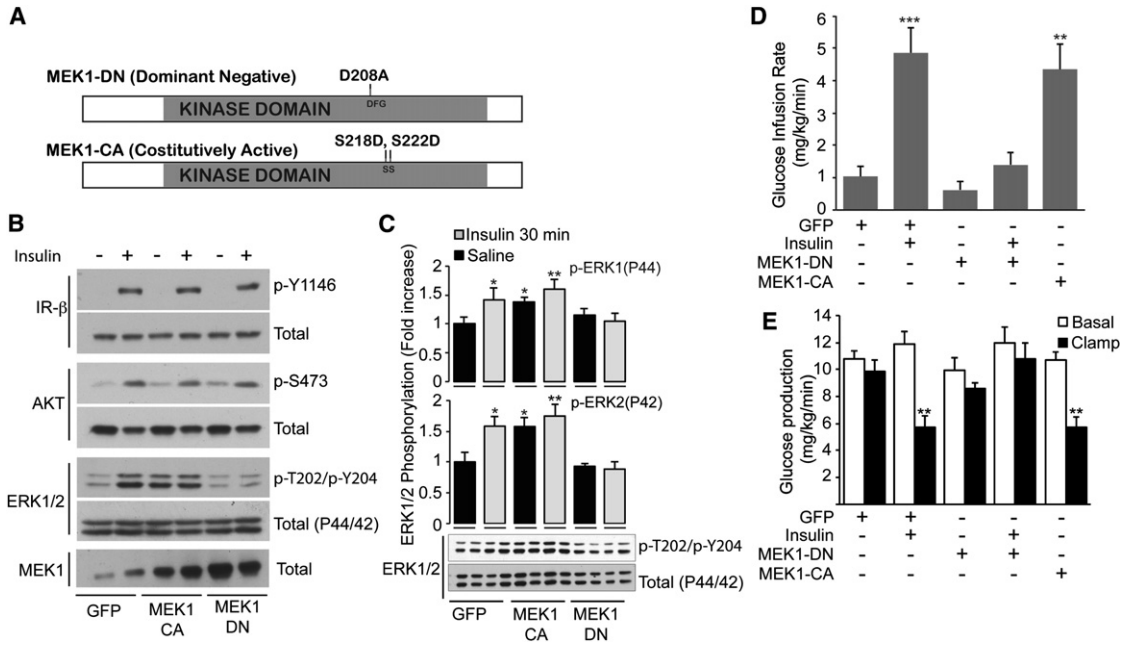

Figure 4. Glucoregulatory Impact of MEK1 Dominant-Negative or Constitutively Active Overexpression in the DVC

(A) The MEK1 diagram is shown with highlighted point mutations that caused its inactivation (MK1-DN, D208A) or the activation (MEK1-CA, S218D, S222D).

(B) HEK293 cells were infected with an adenovirus expressing GFP or active/inactive MEK1. Forty-eight hours postinfection, cells were starved for 16 hr and then treated with insulin (100 nM) for 30 min. Cell lysates were immunoblotted for phospho/total IRβ, AKT, and Erk1/2 and total MEK1.

(C) The adenovirus expressing the MEK1-DN, MEK-CA, or GFP was injected the same day of the stereotactic surgery bilaterally into the DVC. On day 6, a total of 4 μU (2 per site) of insulin was infused for 5 min (0.4 μU/min). The rats were then sacrificed after 30 min. The level of phosphorylation of Erk1/2 was analyzed by western blot. The phosphorylation level was quantified by densitometry and normalized for the total protein. For each condition, n = 5 samples were analyzed. A representative blot is shown. Values are shown as mean + SEM.

(D and E) Pancreatic-euglycemic clamp. Saline or insulin (a total of 2.52 μU, 1.26 μU per site) was infused bilaterally into the DVC at 0.006 μl/min during the clamp through the DVC catheter. (D) Glucose infusion rate (mg/Kg/min) measured during the final 30 min of clamp. (E) Glucose production (mg/Kg/min) in basal (with square) and clamp (black square). Values are shown as mean + SEM n = 6 GFP rats (untreated or insulin-treated), n = 6 MEK1-CA rats, n = 7 MEK1-DN rats treated with insulin, and n = 4 MEK1-DN rats treated with saline. ***p < 0.001, **p < 0.01, *p < 0.05 versus corresponding control.

Glucose uptake remained unchanged (Figure S4B). The glucoregulatory impact of DVC MEK1-CA was comparable to that seen with DVC insulin. Together with the molecular and chemical loss-of-function data, these gain-of-function experiments targeting DVC Erk1/2 signaling suggest that activation of Erk1/2 signaling in the DVC is sufficient and necessary for insulin to inhibit glucose production.

DVC Insulin-Erk1/2 Signaling Activates K_{ATP} Channels to Inhibit Glucose Production

To investigate the potential downstream effectors of insulin-Erk1/2 signaling in the DVC, we first note that insulin activates K_{ATP} channels in hippocampal neurons in an Erk1/2-dependent and PI3K-independent manner in vitro (O'Malley et al., 2003). In parallel, the Kir6.2 subunit of the K_{ATP} channels is phosphorylated by Erk1/2 at T341 and S385 in vitro (Lin and Chai, 2008). Given that the Kir6.2 K_{ATP} channels are highly expressed in the DVC of rat brains (Thomzig et al., 2005) and that activation of the hypothalamic Sur1/Kir6.2 K_{ATP} channels is necessary for insulin to inhibit glucose production (Pocai et al., 2005), we next investigated whether activation of the K_{ATP} channels in the DVC is necessary for insulin-Erk1/2 signaling to inhibit glucose production. To address this possibility, K_{ATP} channel blocker glibenclamide was coinfused with insulin into the DVC while the impact on glucose kinetics was assessed. Coinfusion of glibenclamide with insulin negated the ability of DVC insulin to increase glucose infusion rate (Figure 5A) and lower glucose production (Figures 5B and 5C) with no changes in glucose uptake (Figure 5D). We also inhibited DVC K_{ATP} channels in the presence of direct Erk1/2 activation via MEK-CA. DVC MEK1-CA failed to increase glucose infusion rate (Figure 5A) and lower glucose production (Figures 5B and 5C) in the presence of DVC glibenclamide infusion. DVC glibenclamide alone did not affect glucose metabolism (Figures 5A–5D). Next, we administered K_{ATP} channel opener diazoxide in the DVC and found that DVC diazoxide increased glucose infusion rate (Figure 5A) and lowered glucose production (Figures 5B and 5C) with no changes in glucose uptake (Figure 5D). Thus, activation of K_{ATP} channels is necessary for DVC insulin-Erk1/2 signaling and sufficient to inhibit glucose production.

Previous studies indicate that insulin potentiates NMDA receptor transmission in the rat hippocampus (Christie et al., 1999). Given that activation of NMDA receptor in the DVC is sufficient (Lam et al., 2010a) and necessary for hypothalamic nutrient sensing (Lam et al., 2011) to lower glucose production, these studies raise the possibility that insulin alternatively activates NMDA receptor in the DVC to regulate glucose metabolism. We here inhibited the DVC NMDA receptor with MK801 in the

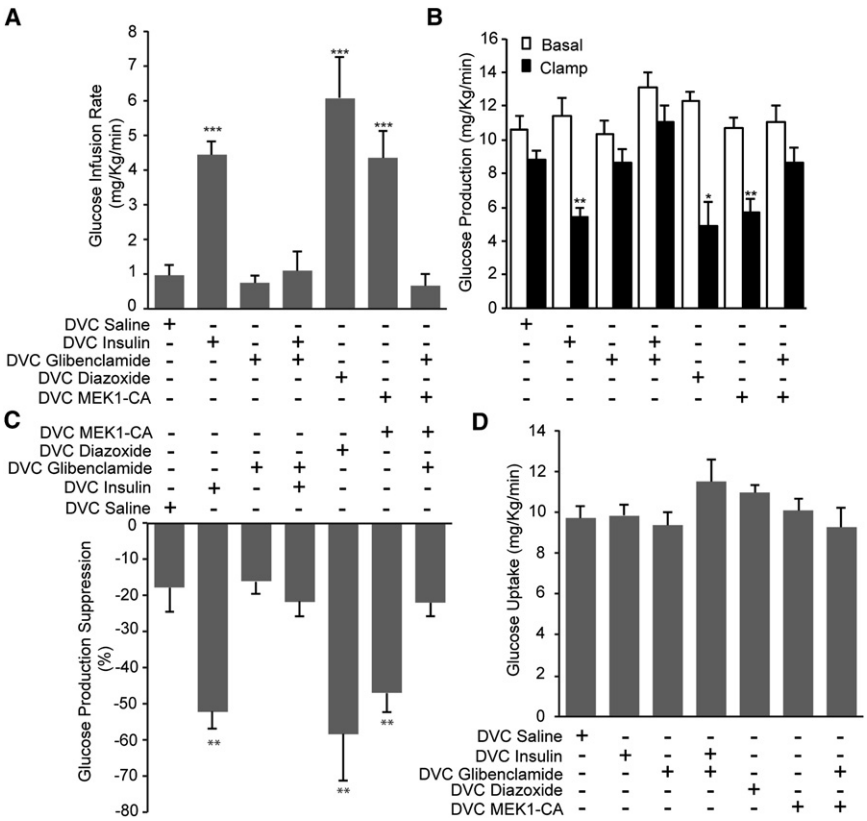

Figure 5. Activation of K_{ATP} Channels in the DVC Is Necessary for Insulin and MEK1-CA and Sufficient to Inhibit Glucose Production

(A–D) A bilateral DVC catheter was implanted on rats (260–280 g) on day 0. The adenovirus expressing the MEK-CA (pfu = 1.7 × 10^8) was injected the same day at 3 μl per site. Venous and arterial cannulations were performed on day 7, and the pancreatic clamp protocol was performed on day 11. Saline, insulin (a total of 2.52 μU, 1.26 μU per site), and diazoxide (46.3 μM) were infused at 0.006 μl/min during the clamp through the DVC catheter. The K_{ATP} channel inhibitor (glibenclamide, 100 μM) was preinfused at 0.006 μl/min for 1 hr before the clamp and infused alone, coinfused with insulin, or infused in MEK1-CA rats during the clamp. Another group of MEK1-CA rats received DVC saline infusion. (A) Glucose infusion rate (mg/Kg/min) measured during the clamp for the indicated treatment. (B) Glucose production (mg/Kg/min) in basal (with square) and clamp (black square) conditions for the indicated treatments. (C) Glucose production suppression (%) induced by the indicated treatments. (D) Glucose uptake was comparable in all groups. Values are shown as mean + SEM of n = 4–6 rats per group. ***p < 0.001, **p < 0.01, *p < 0.05 versus the corresponding controls.

presence of insulin infusion. DVC MK801 failed to negate the ability of DVC insulin to increase glucose infusion rate (Figure S5A) and lower glucose production (Figures S5B and S5C) during the clamps, while glucose uptake remained unchanged (Figure S5D). DVC MK801 alone did not affect glucose metabolism (Figure S5).

These data collectively suggest that DVC insulin-Erk1/2 signals via a K_{ATP} channel-dependent and NMDA receptor-independent pathway to inhibit glucose production.

Circulating Hyperinsulinemia Inhibits Glucose Production through Erk1/2 Signaling in the DVC

To begin addressing the physiological role of DVC Erk1/2 signaling in mediating insulin to regulate glucose homeostasis, we inhibited MAPK-signaling cascades in the DVC while plasma insulin levels were raised by ~3- to 4-fold (Table S3) via a 2 hr hyperinsulinemic-euglycemic clamp (Figure 6A). Circulating hyperinsulinemia increased glucose infusion rate (Figure 6B) required to maintain euglycemia (Table S1). This corresponded to an inhibition of glucose production (Figures 6C and 6E) and a stimulation of glucose uptake (Figure 6D). In the presence of DVC Erk1/2 signaling inhibition (via PD98069), the glucose infusion rate was reduced during the hyperinsulinemic-euglycemic clamps (Figure 6B). The ability of insulin to stimulate glucose uptake remained intact (Figure 6D) while the suppression of glucose production was partly prevented (Figures 6C and 6E). Thus, a direct disruption of Erk1/2 signaling in the DVC impairs circulating hyperinsulinemia to inhibit glucose production and may thereby lead to hepatic insulin resistance.

High-Fat Feeding Induces Insulin Resistance in the DVC, while DVC Insulin Resistance Is Bypassed by Direct Activation of DVC K_{ATP} Channels

High-fat diet (HFD) feeding of rats induces hepatic insulin resistance (Wang et al., 2001), due partly to a disruption of hypothalamic insulin action (Ono et al., 2008). To test whether HFD induces insulin resistance in extra-hypothalamic regions such as the DVC, we fed rats with HFD for 3 days and first infused insulin (2 μU/site) and analyzed the level of Erk1/2 activation in the DVC (Figure 7A). We then tested the glucoregulatory effect of DVC insulin in HFD rats via the use of the pancreatic clamp (Figure 7B). Consistent with previous findings (Figure 1C and Figure S1D), DVC insulin activated Erk1/2 in normal rats, but instead failed to activate Erk1/2 in HFD rats (Figure 7A). There was a significant increase of basal DVC Erk2 activation in HFD-fed rats, but DVC insulin did not further activate Erk2 (Figure 7A). Importantly, the failure of DVC insulin to activate Erk1/2 signaling was associated with the inability of DVC insulin infusion to increase glucose infusion rate (Figure 7C) and lower glucose production (Figure 7D and Figure S6B) during the clamps in HFD rats with no changes in glucose uptake (Figure S6A). However, when we tested whether activation of DVC Erk1/2 signaling could bypass insulin resistance by directly injecting MEK1-CA into the DVC of HFD rats, DVC MEK1-CA failed to lower glucose production (data not shown).

Lastly, given that activation of the K_{ATP} channels in the DVC is necessary for insulin-Erk1/2 and sufficient to inhibit glucose production in normal rats (Figure 5), we directly infused diazoxide into the DVC of HFD rats. DVC diazoxide increased glucose

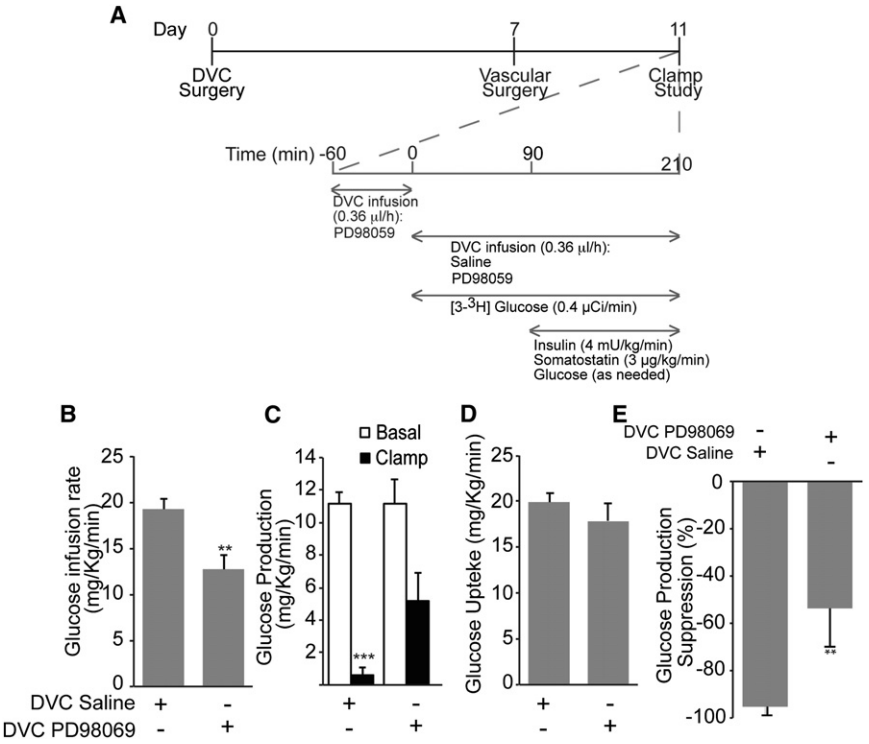

Figure 6. Direct Disruption of ERK1/2 Signaling in the DVC Negates the Ability of Circulating Insulin to Inhibit Glucose Production

(A) Experimental procedure and hyperinsulinemic clamp protocol. Saline or the MEK1/2 inhibitor (PD98059, 100 μM) was preinfused at 0.006 μl/min for 1 hr before the clamp and then during the clamp at the same rate through the DVC catheter.

(B) Glucose infusion rate (mg/Kg/min) measured during the 30 min of the clamp.

(C) Glucose production (mg/Kg/min) in basal (with square) and clamp (black square) conditions.

(D) Glucose uptake was comparable in all groups.

(E) Glucose production suppression (%) induced by the indicated treatments. Values are shown as mean + SEM of n = 7 for both saline and PD98059 treatments. ***p < 0.001, **p < 0.01, *p < 0.05 versus corresponding control.

infusion rate (Figure 7C) and inhibited glucose production (Figure 7D and Figure S6B) in HFD rats to a similar extent as in normal rats (Figure 5). Together, these data suggest that activation of DVC K_{ATP} channels, but not Erk1/2 signaling, is sufficient to bypass insulin resistance to lower glucose production in HFD rats.

DISCUSSION

The metabolic impact of insulin action in the brain has generated considerable interest in recent decades. In rodents, insulin action in the hypothalamus regulates peripheral glucose (Koch et al., 2008; Könner et al., 2007b; Obici et al., 2002; Pocai et al., 2005) and lipid (Scherer et al., 2011; Koch et al., 2008) homeostasis, as well as food intake and body weight (Schwartz and Porte, 2005). The clinical relevance of insulin action in the brain is becoming apparent as intranasal delivery of insulin reduces food intake and plasma glucose levels in normal humans (Hallschmid et al., 2012; Filippi et al., 2012). Intranasal insulin delivery does not limit site of insulin action to the hypothalamus, suggesting that extra-hypothalamic sites remain possible targets for insulin. The current study reveals DVC as a responsive region to insulin to regulate glucose production in both rats and mice. Contrary to insulin action in the hypothalamus, insulin in the DVC triggers a PI3K-independent pathway to regulate glucose production. Insulin infusion into the DVC fails to activate PI3K and AKT, while the same dose of insulin is sufficient to activate PI3K and AKT in the hypothalamus. In addition, direct infusion of PI3K inhibitors into the DVC fails to negate the glucoregulatory effect of insulin, while the same dose of inhibitors given into the third ventricle is sufficient to abolish the effect of central insulin. Although the insulin signaling pathway that mediates insulin's ability to inhibit glucose production in both the DVC and MBH diverges, the downstream effector appears to be the same as infusion of the K_{ATP} channel blocker into the DVC (like in MBH, Pocai et al., 2005) abolishes the ability of insulin to inhibit glucose production. These findings imply that direct activation of K_{ATP} channels in the brain, which lowers glucose production in humans (Kishore et al., 2011), may not be limited to the K_{ATP} channels expressed in the hypothalamus, but also the ones expressed in the DVC. Nonetheless, an important question remains as to how DVC insulin activates K_{ATP} channel.

Consistent with the fact that insulin activates K_{ATP} channel in an Erk1/2-dependent manner in the hippocampal neurons (O'Malley et al., 2003), DVC insulin administration activates Erk1/2 signaling and K_{ATP} channels in association with an inhibition of glucose production. Importantly, molecular and chemical inhibition of Erk1/2 upstream kinase MEK1 negates the ability of DVC insulin to activate Erk1/2 and inhibit glucose production, while molecular activation of MEK1 in the DVC is sufficient to recapitulate the effect of insulin to activate Erk1/2 and K_{ATP} channels and inhibit glucose production. Given that the activation of K_{ATP} channels in the hypothalamus mediates not only insulin but also nutrients to regulate glucose homeostasis (Lam, 2010b; Yue and Lam, 2012), the current findings raise the possibility that nutrient-related signals activate DVC K_{ATP} channels to regulate glucose homeostasis. This hypothesis remains to be tested. Although the direct delivery of insulin into the DVC is potentially pharmacological in nature, the physiological relevance of insulin action in the DVC is demonstrated when a direct disruption of DVC Erk1/2 signaling negates the ability of circulating hyperinsulinemia to inhibit glucose production. Together with the ability of the hypothalamus to sense circulating insulin to regulate glucose production, these data illustrate that insulin action in the DVC and the MBH may exhibit redundant, but yet different, sensing mechanisms to mediate insulin's ability to inhibit glucose production.

To date, it is believed that the metabolic effect of insulin on glucose regulation in insulin-sensitive tissues such as muscle,

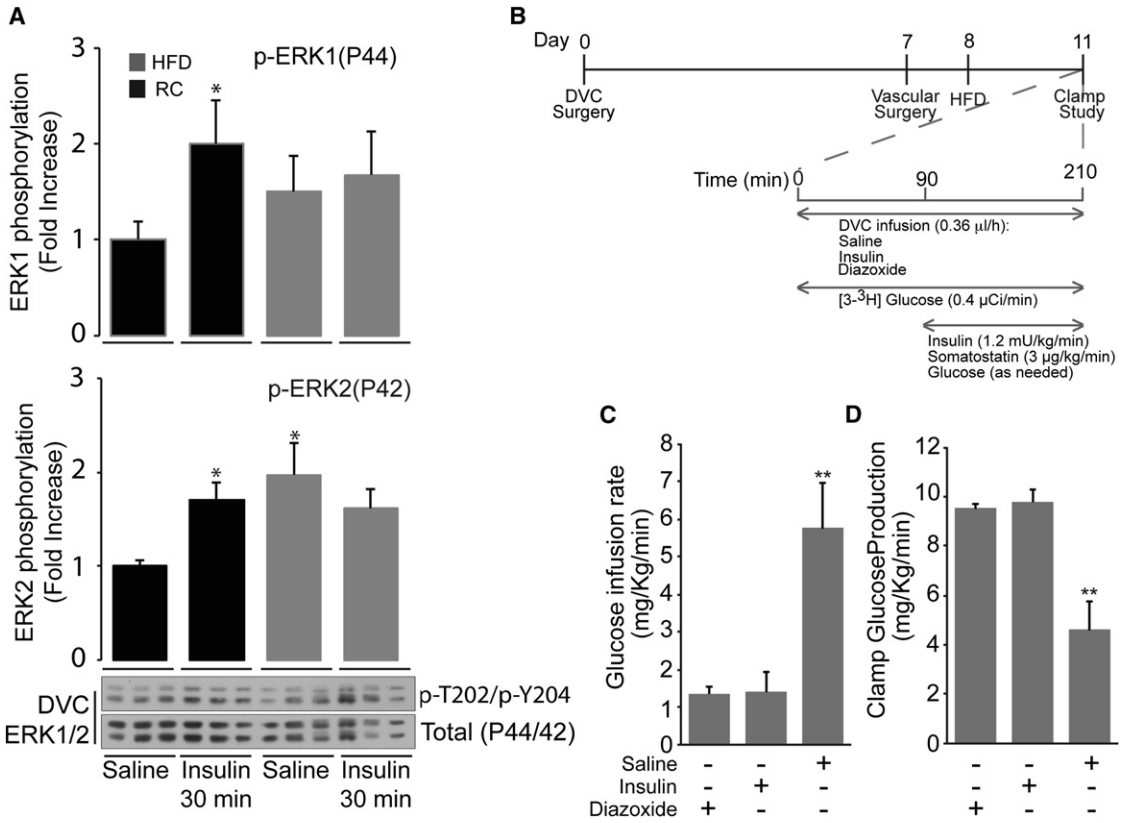

Figure 7. HFD Induces Insulin Resistance in the DVC, while DVC Insulin Resistance Is Bypassed by Direct DVC K_{ATP} Channel Activation

(A) A bilateral DVC catheter was implanted on rats (260–280 g) on day 0. On day 3 the rats were put on HFD or RC, and on day 6, a total of 4 μU (2 per site) of insulin was infused for 5 min (0.2 μl/min). The rats were then sacrificed after 30 min. The level of phosphorylation of Erk1/2 was analyzed by western blot. The phosphorylation level was quantified by densitometry and normalized for the total protein. For each condition at least n = 5 samples were analyzed. Data are presented as fold increase over the RC saline-treated samples. A representative blot is also shown.

(B) Experimental procedure and clamp protocol of 3 days HFD-fed rats. Saline, insulin (a total of 2.52 μU, 1.26 μU per site), and diazoxide (46.3 μM) were infused at 0.006 μl/min during the clamp through the DVC catheter.

(C) Glucose infusion rate (mg/Kg/min) measured during the clamp.

(D) Glucose production during the clamp (mg/Kg/min). Values are shown as mean + SEM n = 4–6 rats for saline, insulin, and diazoxide treatments. $^{**}p < 0.01$, $^{*}p < 0.05$ versus corresponding control.

adipocytes, liver, and the hypothalamus is mediated by a PI3K-dependent and MAP-kinase-independent mechanisms (Gabbay et al., 1996; Obici et al., 2002; Saltiel and Kahn, 2001). To our surprise, our findings contrarily illustrate that insulin triggers an Erk1/2 signaling-dependent but PI3K-independent mechanism in the DVC to activate K_{ATP} channels and inhibit glucose production in vivo. Although the underlying preferential mechanism(s) of insulin to activate MEK1/2 over PI3K in the DVC remain to be clarified, we postulate that insulin in the DVC activates Erk1/2 signaling to phosphorylate the Kir6.2 subunit of the K_{ATP} channels at T341 and S385 (Lin and Chai, 2008) and lowers glucose production. This working hypothesis remains to be tested.

The DVC consists of various nuclei such as the nucleus of the solitary tract (NTS), the area postrema, and the dorsal motor nucleus of the vagus. Although our current DVC surgical procedure targets the infusate to the NTS and suggests that insulin action in the NTS lowers glucose production, future studies are warranted to characterize and compare insulin signaling and the associated metabolic impacts in each of the nuclei within the DVC. In addition, the role of the sympathetic and/or parasympathetic output pathways that may mediate the ability of DVC insulin to regulate glucose production remains to be clarified.

High-fat feeding induces insulin resistance at the level of peripheral tissues as well as the hypothalamus. The current study pinpoints insulin resistance in the DVC as an additional site of signaling impairment induced by high-fat feeding. Interestingly, in contrast to peripheral tissues and the hypothalamus, where a disruption in PI3K activity is primarily responsible for the inability of insulin to regulate glucose metabolism, high-fat feeding impairs the ability of insulin to activate Erk1/2 signaling in the DVC and inhibit glucose production. However, direct activation of Erk1/2 signaling in the DVC still fails to inhibit glucose production in response to high-fat feeding, while DVC K_{ATP} channel activation is equally potent in both normal and HFD rats to inhibit glucose production. These findings indicate that diet-induced DVC insulin resistance lies in the inability of Erk1/2 signaling to activate K_{ATP} channels. In light of the fact that direct activation of K_{ATP} channels in the DVC bypasses insulin resistance to inhibit glucose production in high-fat-fed rats

(current study), oral diazoxide treatment may be equally potent to inhibit glucose production in normal humans (Kishore et al., 2011) and in individuals with obesity and diabetes. This working hypothesis remains to be tested.

In summary, we here unveil that insulin normally triggers an Erk1/2-depenedent but PI3K-independent pathway in the DVC to inhibit glucose production. Importantly, high-fat feeding disrupts the insulin-Erk1/2 signaling axis in the DVC to inhibit glucose production, thereby revealing a previously unappreciated site of insulin resistance induced by high-fat feeding.

EXPERIMENTAL PROCEDURES

Materials

Antibodies anti-IRβ (total and p-Y1146), AKT (total, p-T308 and p-S473), ERK1/2 (total and p-T202/Y204), IRS-1 (total and p-Y895), and MEK1 (total) were from Cell Signaling Technology (Danvers, MA). The anti-p89 PI3K subunit antibody and the anti-phospho-IRS-1 (p-Y608) antibodies were from Millipore (Billerica, MA). The Pierce ECL Western Blotting Substrate was from Thermo Scientific (Rockford, IL). Radioactive [3-^{3}H]glucose was from PerkinElmer (Boston, MA). Mutagenesis/PCR cloning primers were from ACGT Corp (Wheeling, IL). The sequence analysis was performed by the TCAG Sequencing Facility (Hospital for Sick Children, Toronto, ON). LY294002, wortmannin, PD98059, glibenclamide, diazoxide, and insulin were from Sigma-Aldrich (St. Louis, MO). The cDNA for MEK1 was in a p-express clone from Genome Club (BioScience imaGene). HEK293T cells were from the American Type Culture Collection (ATCC).

Animal Preparation

Eight-week-old male Sprague-Dawley rats weighing between 260 and 280 g and 18-week-old male C57/B6 mice weighing between 25 and 30 g (Charles River Laboratories, Montreal, QC) were used for our studies. Rats and mice were housed in individual cages and maintained on a standard light-dark cycle with access to standard rat/mice chow and water ad libitum. Rats were stereotaxically (David Kopf Instruments, Tujunga, CA) implanted with indwelling bilateral catheters targeting the mediobasal hypothalamus (MBH) (3.1 mm posterior of bregma, 0.4 mm lateral from midline, and 9.6 mm below skull surface) (Lam et al., 2011) and the nucleus of the solitary tract (NTS) within the DVC (0.0 mm on occipital crest, 0.4 mm lateral to midline, and 7.9 mm below skull surface) (Lam et al., 2010a). After 1 week of recovery, rats underwent intravenous catheterization where the internal jugular vein and carotid artery were catheterized for infusion and sampling. Mice were stereotaxically (David Kopf Instruments) implanted with indwelling catheters in the fourth ventricle (6 mm posterior of bregma and 4 mm below the skull). After a week of recovery, mice underwent intravenous catheterization where the internal jugular vein was catheterized for infusion. All study protocols were reviewed and approved by the Institutional Animal Care and Use Committee of the University Health Network.

DVC/MBH Infusion for Signaling Study

A bilateral DVC or MBH catheter was implanted on day 0 on male Sprague-Dawley rats (260–280 g) as described above. On day 5, the rats were restricted to 15 g (50.7 cal for RC and 77.1 cal for HFD) of food for the night, and on day 6, a total of 4 μU (2 per site) of insulin (Ono et al., 2008) was infused for 5 min (0.4 μU/min). The MEK1/2 inhibitor (PD98059, 200 μM) was preinfused at 0.2 μl/min for 5 min and 1 hr before the insulin treatment, and then coinfused with insulin. The rats were then sacrificed after 30 or 40 min, and the DVC or MBH tissue was immediately collected. Tissues (~12 mg) were lysed with a handheld glass homogenizer in a buffer containing 50 mM Tris-HCl (pH 7.5), 1 mM EGTA, 1 mM EDTA, 1% (w/v) Nonidet P40, 1 mM sodium orthovanadate, 50 mM sodium fluoride, 5 mM sodium pyrophosphate, 0.27 M sucrose, 1 μM Dithiotritolo (DTT), and protease inhibitor cocktail (Roche). Protein concentration of each homogenized tissue was determined with the Pierce 660 nm protein assay (Thermo Scientific).

Western Blotting

Between 10 and 20 μg of tissue lysates obtained as described above were subjected to electrophoresis on a 10% polyacrylamide gel and transferred to nitrocellulose membranes. The membranes were incubated for 1 hr with TBS-T containing 5% (w/v) BSA. The membranes were then immunoblotted in the same buffer for 16 hr at 4°C with the indicated primary antibodies diluted to 1000-fold. The blots were then washed four times with TBS-T and incubated with secondary HRP-conjugated antibodies in 5% skimmed milk. After repeating the washing steps, the signal was detected with the enhanced chemiluminescence reagent (ECL). Immunoblots were developed using a film automatic processor (SRX-101; Konica Minolta Medical), and films were scanned with 300 dpi resolution on a scanner (PowerLook 1000; UMAX). The phosphorylation level of the Irβ, AKT, IRS-1, and Erk1/2 was quantified by densitometry with the ImageJ software and normalized for the corresponding total protein level.

PI3K Activity Assay

The activity of the MBH/DVC PI3K was measured with the PI3K activity ELISA: Pico kit (echelon, K-1000s; Salt Lake City, UT). Briefly, the PI3K was immunoprecipitated from 500 μg of the tissue lysate produced upon DVC/MBH infusion (as described above) with 5 μl of an anti-p89 PI3K subunit antibody (Millipore). The lysate was incubated for 1 hr at 4°C in a rotating wheel with the antibody, and then 25 μl of 25% protein A/G beads were added (Santa Cruz) and the lysate was incubated for an additional hour at 4°C in a rotating wheel. The beads were then washed three times with the lysis buffer (see above) + 0.1M NaCl; three times with 0.1 M Tris-HCl (pH 7.4), 5 mM LiCl, and 0.1 mM sodium orthovanadate; and twice with 10 mM Tris-HCl (pH 7.4), 150 mM NaCl, 5 mM EDTA, and 0.1 mM sodium orthovanadate. The beads were then resuspended in the KBZ reaction buffer provided by the kit. The Production of $PI(3,4,5)P_2$ was measured according to the manufacturer instructions. Data are presented as fold increase over the saline-treated samples. Values are shown as mean + SEM significant with a p value of < 0.05 versus corresponding control.

DVC Infusion and Pancreatic-Euglycemic/Hyperinsulinemic Clamp in Rats

Four days after intravenous catheterization, animals whose food intake and body weight had recovered back to within 10% of baseline underwent the clamp studies. Rats were restricted to 15 g (50.7 cal for RC and 77.1 cal for HFD) of food the night before the experiment to ensure the same nutritional status during the clamps, which lasted 210 min. Saline, insulin (a total of 1.26 μU per site), or the K_{ATP} channel activator (diaxozide, 56 pmols per site) were infused at 0.006 μl/min during the clamp (from time 0 to 210) through the DVC catheter. The insulin receptor antagonist (S961, 1.3 μg/μl) (Schäffer et al., 2008; Paranjape et al., 2010), the PI3K inhibitors (LY294002, 16.2 pmols per site and wortmannin, 3.2 pmols per site), the MEK1/2 inhibitor (PD98059, 0.156 nmols per site), and the K_{ATP} channel inhibitor (glibenclamide, 0.156 nmols per site) were preinfused at 0.006 μl/min for 1 hr before the clamp (time 60) and infused or coinfused with insulin during the clamp. A primed-continuous intravenous infusion of [3-^{3}H]glucose (40 μCi bolus, 0.4 μCi/min) was also initiated at 0 min and maintained throughout the study to assess glucose kinetics. A pancreatic (basal insulin)-euglycemic clamp was started at time 90 min until 210 min. Somatostatin (3 μg/kg/min) was infused intravenously along with insulin (1.2 mU/kg/min) to replace insulin back to basal. A 25% glucose solution was started at time 90 and periodically adjusted to maintain plasma glucose levels. For the hyperinsulinemic clamp, insulin was intravenously infused at 4 mU/Kg/min. Samples for the determination of [3-^{3}H] glucose-specific activity and insulin (see Tables S1 and S2) levels were obtained at 10 min intervals. At the end, the rats were sacrificed and samples of MBH and DVC tissue were taken as previously reported (Lam et al., 2011). The brain insulin and PI3K or MEK1/2 inhibitor concentrations were chosen as previously described (Obici et al., 2002), while the concentration of the glibenclamide and diazoxide was the same as previously reported (Pocai et al., 2005).

Fourth Ventricle Infusion and Pancreatic-Euglycemic Clamp in Mice

A cannula was implanted in the fourth ventricle of male mice on day 0, and venous and arterial cannulations were performed on day 7. The pancreatic

clamp was performed on day 9. Saline or insulin (4.08 μU total) was preinfused at 0.017 μl/min for 1 h 30 min before the clamp and then during the clamp through catheters. A primed-continuous intravenous infusion of [3-^{3}H]glucose (1 μCi bolus, 0.1 μCi/min; Perkin Elmer) was also initiated at 0 min and maintained throughout the study to assess glucose kinetics. A pancreatic (basal insulin)-euglycemic clamp was started at time 60 min until 150 min. Somatostatin (8.3 μg/kg/min) was infused along with insulin (1.4 mU/kg/min) to replace insulin back to basal. A 10% glucose solution was started at time 60 and periodically adjusted to maintain plasma glucose levels. Samples for the determination of [3-^{3}H]glucose-specific activity were obtained at 10 min intervals.

Preparation and Injection of MEK1 Dominant-Negative and Constitutively Active Adenovirus in Rats

Rat MEK1 cDNA wild-type was mutated in the magnesium binding site (D208 mutated to A) to kill the catalytic activity (MEK1-DN) and in the two activatory serines (S218 and S222 mutated to D) to enhance the catalytic activity (MEK1-CA). Cloning, restriction enzyme digests, DNA ligations, and other recombinant DNA procedures were performed using standard protocols. All site-directed mutagenesis reactions were performed using KOD polymerase (Novagen) followed by digestion of the product with DpnI. Mutated cDNA was subcloned in the pacAd5 CMV shuttle vector of the RAPAd CMV Adenoviral Expression System (Cell Biolabs, Inc., San Diego, CA). The adenovirus was produced in HEK293 cells by cotransfecting the PAC1 linearized RAPAd Ad Backbone vector with the pacAd5 CMV shuttle vector carrying the cDNA for MEK1-DN or MEK-CA or GFP according to the manufacturer's instructions. Purified adenoviruses with pfu of 1.8×10^8 (MEK1-DN), 1.7×10^8 (MEK1-CA), or 3×10^8 (GFP) were injected the same day of the DVC brain surgery at 3 μl per site.

HEK293 Viral Infection and Insulin Treatment

A total of 1×10^6 HEK293 cells were plated in a 6-well plate and infected the day after with an adenovirus expressing GFP or active/inactive MEK1. Forty-eight hours postinfection, cells were starved for 16 hr and then treated with insulin (100 nM) for 30 min. Cells were then lysed in a buffer containing 50 mM Tris-HCl (pH 7.5), 1 mM EGTA, 1 mM EDTA, 1% (w/v) Nonidet P40, 1 mM sodium orthovanadate, 50 mM sodium fluoride, 5 mM sodium pyrophosphate, 0.27 M sucrose, 1 μM Dithiotritolo (DTT), and protease inhibitor cocktail (Roche). Twenty micrograms of lysates were immunoblotted for phospho/total IRβ, AKT, and Erk1/2 and total MEK1 (as described above).

Biochemical Analysis

Plasma glucose concentrations were measured by the glucose oxidase method (Glucose Analyzer GM9; Analox Instruments, Lunenbertg, MA). Plasma insulin levels were determined by radioimmunoassay (RIA) (Linco Research, St. Charles, MO).

Statistical Analysis

Statistical analysis was done with GraphPad Prism by one-way ANOVA to compare across the groups, followed by a Tukey's post hoc test or t test where appropriate to compare between groups. Statistical analysis was accepted as significant with a p value of < 0.05. Data are presented as means + SEM.

SUPPLEMENTAL INFORMATION

Supplemental Information includes six figures and three tables and can be found with this article online at http://dx.doi.org/10.1016/j.cmet.2012.09.005.

ACKNOWLEDGMENTS

We thank P. Wang for her excellent technical assistant and Dr. Schäffer from Novo Dordisk for kindly providing us with the insulin receptor antagonist (S961). This work was supported by a grant from the Canadian Diabetes Association (OG-3-10-3048-TL). B.M.F. is supported by an Early Researcher Award from the Ontario Ministry of Research and Innovation (ER08-05-141, awarded to T.K.T.L.). C.S.Y. was supported by graduate scholarships from the Canadian Institute of Health Research and the University of Toronto Banting and Best Diabetes Centre. T.K.T.L. holds the John Kitson McIvor (1915-1942) Endowed Chair in Diabetes Research and the Canada Research Chair in Obesity at the Toronto General Research Institute and the University of Toronto.

Received: March 30, 2012
Revised: August 1, 2012
Accepted: September 11, 2012
Published online: October 2, 2012

REFERENCES

Agarwala, G.C., Mittal, R.K., Bapat, S.K., and Bhardwaj, U.R. (1977). Effect of centrally administered insulin on blood glucose levels in dogs. Indian J. Physiol. Pharmacol. *21*, 11–18.

Breen, D.M., Rasmussen, B.A., Kokorovic, A., Wang, R., Cheung, G.W., and Lam, T.K. (2012). Jejunal nutrient sensing is required for duodenal-jejunal bypass surgery to rapidly lower glucose concentrations in uncontrolled diabetes. Nat. Med. *18*, 950–955.

Cheung, G.W., Kokorovic, A., Lam, C.K., Chari, M., and Lam, T.K. (2009). Intestinal cholecystokinin controls glucose production through a neuronal network. Cell Metab. *10*, 99–109.

Chowers, I., Lavy, S., and Halpern, L. (1966). Effect of insulin administered intracisternally on the glucose level of the blood and the cerebrospinal fluid in vagotomized dogs. Exp. Neurol. *14*, 383–389.

Christie, J.M., Wenthold, R.J., and Monaghan, D.T. (1999). Insulin causes a transient tyrosine phosphorylation of NR2A and NR2B NMDA receptor subunits in rat hippocampus. J. Neurochem. *72*, 1523–1528.

Coll, A.P., Farooqi, I.S., and O'Rahilly, S. (2007). The hormonal control of food intake. Cell *129*, 251–262.

Cummings, D.E., and Overduin, J. (2007). Gastrointestinal regulation of food intake. J. Clin. Invest. *117*, 13–23.

Defronzo, R.A. (2009). Banting Lecture. From the triumvirate to the ominous octet: a new paradigm for the treatment of type 2 diabetes mellitus. Diabetes *58*, 773–795.

Filippi, B.M., Mighiu, P.I., and Lam, T.K. (2012). Is insulin action in the brain clinically relevant? Diabetes *61*, 773–775.

Gabbay, R.A., Sutherland, C., Gnudi, L., Kahn, B.B., O'Brien, R.M., Granner, D.K., and Flier, J.S. (1996). Insulin regulation of phosphoenolpyruvate carboxykinase gene expression does not require activation of the Ras/mitogen-activated protein kinase signaling pathway. J. Biol. Chem. *271*, 1890–1897.

Gelling, R.W., Morton, G.J., Morrison, C.D., Niswender, K.D., Myers, M.G., Jr., Rhodes, C.J., and Schwartz, M.W. (2006). Insulin action in the brain contributes to glucose lowering during insulin treatment of diabetes. Cell Metab. *3*, 67–73.

Grill, H.J. (2006). Distributed neural control of energy balance: contributions from hindbrain and hypothalamus. Obesity (Silver Spring) *14* (*Suppl 5*), 216S–221S.

Hallschmid, M., Higgs, S., Thienel, M., Ott, V., and Lehnert, H. (2012). Postprandial administration of intranasal insulin intensifies satiety and reduces intake of palatable snacks in women. Diabetes *61*, 782–789.

Kishore, P., Boucai, L., Zhang, K., Li, W., Koppaka, S., Kehlenbrink, S., Schiwek, A., Esterson, Y.B., Mehta, D., Bursheh, S., et al. (2011). Activation of K(ATP) channels suppresses glucose production in humans. J. Clin. Invest. *121*, 4916–4920.

Koch, L., Wunderlich, F.T., Seibler, J., Könner, A.C., Hampel, B., Irlenbusch, S., Brabant, G., Kahn, C.R., Schwenk, F., and Brüning, J.C. (2008). Central insulin action regulates peripheral glucose and fat metabolism in mice. J. Clin. Invest. *118*, 2132–2147.

Könner, A.C., Janoschek, R., Plum, L., Jordan, S.D., Rother, E., Ma, X., Xu, C., Enriori, P., Hampel, B., Barsh, G.S., et al. (2007a). Insulin action in AgRP-expressing neurons is required for suppression of hepatic glucose production. Cell Metab. *5*, 438–449.

Könner, A.C., Janoschek, R., Plum, L., Jordan, S.D., Rother, E., Ma, X., Xu, C., Enriori, P., Hampel, B., Barsh, G.S., et al. (2007b). Insulin action in AgRP-

expressing neurons is required for suppression of hepatic glucose production. Cell Metab. *5*, 438–449.

Lam, T.K. (2010b). Neuronal regulation of homeostasis by nutrient sensing. Nat. Med. *16*, 392–395.

Lam, C.K., Chari, M., Su, B.B., Cheung, G.W., Kokorovic, A., Yang, C.S., Wang, P.Y., Lai, T.Y., and Lam, T.K. (2010a). Activation of N-methyl-D-aspartate (NMDA) receptors in the dorsal vagal complex lowers glucose production. J. Biol. Chem. *285*, 21913–21921.

Lam, C.K., Chari, M., Rutter, G.A., and Lam, T.K. (2011). Hypothalamic nutrient sensing activates a forebrain-hindbrain neuronal circuit to regulate glucose production in vivo. Diabetes *60*, 107–113.

Lin, Y.F., and Chai, Y. (2008). Functional modulation of the ATP-sensitive potassium channel by extracellular signal-regulated kinase-mediated phosphorylation. Neuroscience *152*, 371–380.

Morton, G.J., Blevins, J.E., Williams, D.L., Niswender, K.D., Gelling, R.W., Rhodes, C.J., Baskin, D.G., and Schwartz, M.W. (2005). Leptin action in the forebrain regulates the hindbrain response to satiety signals. J. Clin. Invest. *115*, 703–710.

Niu, S.N., Huang, Z.B., Wang, H., Rao, X.R., Kong, H., Xu, J., Li, X.J., Yang, C., and Sheng, G.Q. (2011). Brainstem Hap1-Ahi1 is involved in insulin-mediated feeding control. FEBS Lett. *585*, 85–91.

O'Malley, D., Shanley, L.J., and Harvey, J. (2003). Insulin inhibits rat hippocampal neurones via activation of ATP-sensitive K+ and large conductance Ca2+-activated K+ channels. Neuropharmacology *44*, 855–863.

Obici, S., Zhang, B.B., Karkanias, G., and Rossetti, L. (2002). Hypothalamic insulin signaling is required for inhibition of glucose production. Nat. Med. *8*, 1376–1382.

Ono, H., Pocai, A., Wang, Y., Sakoda, H., Asano, T., Backer, J.M., Schwartz, G.J., and Rossetti, L. (2008). Activation of hypothalamic S6 kinase mediates diet-induced hepatic insulin resistance in rats. J. Clin. Invest. *118*, 2959–2968.

Paranjape, S.A., Chan, O., Zhu, W., Horblitt, A.M., McNay, E.C., Cresswell, J.A., Bogan, J.S., McCrimmon, R.J., and Sherwin, R.S. (2010). Influence of insulin in the ventromedial hypothalamus on pancreatic glucagon secretion in vivo. Diabetes *59*, 1521–1527.

Pocai, A., Lam, T.K., Gutierrez-Juarez, R., Obici, S., Schwartz, G.J., Bryan, J., Aguilar-Bryan, L., and Rossetti, L. (2005). Hypothalamic K(ATP) channels control hepatic glucose production. Nature *434*, 1026–1031.

Ramnanan, C.J., Saraswathi, V., Smith, M.S., Donahue, E.P., Farmer, B., Farmer, T.D., Neal, D., Williams, P.E., Lautz, M., Mari, A., et al. (2011). Brain insulin action augments hepatic glycogen synthesis without suppressing glucose production or gluconeogenesis in dogs. J. Clin. Invest. *121*, 3713–3723.

Saltiel, A.R., and Kahn, C.R. (2001). Insulin signalling and the regulation of glucose and lipid metabolism. Nature *414*, 799–806.

Schäffer, L., Brand, C.L., Hansen, B.F., Ribel, U., Shaw, A.C., Slaaby, R., and Sturis, J. (2008). A novel high-affinity peptide antagonist to the insulin receptor. Biochem. Biophys. Res. Commun. *376*, 380–383.

Scherer, T., O'Hare, J., Diggs-Andrews, K., Schweiger, M., Cheng, B., Lindtner, C., Zielinski, E., Vempati, P., Su, K., Dighe, S., et al. (2011). Brain insulin controls adipose tissue lipolysis and lipogenesis. Cell Metab. *13*, 183–194.

Schwartz, M.W., and Porte, D., Jr. (2005). Diabetes, obesity, and the brain. Science *307*, 375–379.

Sun, X.J., and Liu, F. (2009). Phosphorylation of IRS proteins Yin-Yang regulation of insulin signaling. Vitam. Horm. *80*, 351–387.

Thomzig, A., Laube, G., Prüss, H., and Veh, R.W. (2005). Pore-forming subunits of K-ATP channels, Kir6.1 and Kir6.2, display prominent differences in regional and cellular distribution in the rat brain. J. Comp. Neurol. *484*, 313–330.

Wang, J., Obici, S., Morgan, K., Barzilai, N., Feng, Z., and Rossetti, L. (2001). Overfeeding rapidly induces leptin and insulin resistance. Diabetes *50*, 2786–2791.

Wang, P.Y., Caspi, L., Lam, C.K., Chari, M., Li, X., Light, P.E., Gutierrez-Juarez, R., Ang, M., Schwartz, G.J., and Lam, T.K. (2008). Upper intestinal lipids trigger a gut-brain-liver axis to regulate glucose production. Nature *452*, 1012–1016.

Yue, J.T., and Lam, T.K. (2012). Lipid sensing and insulin resistance in the brain. Cell Metab. *15*, 646–655.